

Performance analysis of hybrid bio-inspired algorithms for classifying brain tumors in imbalanced magnetic resonance imaging datasets

Rahul Ramesh Chakre¹, Archana S. Vaidya², Dipak V. Patil²

¹School of Computational Sciences, Faculty of Science and Technology, JSPM University Pune, Pune, India

²GES's R. H. Sapat College of Engineering, Management Studies and Research, Nashik, Savitribai Phule Pune University, Pune, India

Article Info

Article history:

Received Sep 9, 2023

Revised Jul 16, 2024

Accepted Aug 6, 2024

Keywords:

Bio-inspired computing
Brain tumor classification
Imbalanced medical image dataset
Immune computing
Swarm intelligence

ABSTRACT

Magnetic resonance imaging (MRI) is a substantial imaging procedure for diagnosing brain tumors. However, brain tumor classification continues challenging due to the unequal distribution of classes within datasets, complicating precise diagnosis and classification. This research focuses on the class imbalance in medical image datasets by proposing a hybrid bio-inspired algorithm for brain tumor classification. A rider optimization and particle rider mutual information-based dendritic-squirrel search algorithm combined with an artificial immune classifier is developed and tested on imbalanced datasets generated from BRATS and SimBRATS. Experimental outcomes are encouraging. For the imbalanced BRATS dataset, the rider optimization-based classifier achieved an accuracy of 94.84%, sensitivity of 92.96%, and specificity of 94.95%. The particle rider mutual information-based classifier outperformed others with 96.25% accuracy, 94.33% sensitivity, and 94.85% specificity. For the imbalanced SimBRATS dataset, the rider optimization-based classifier achieved 94.95% accuracy, 92.05% sensitivity, and 94.04% specificity. The particle rider mutual information-based classifier excelled with 96.35% accuracy, 94.42% sensitivity, and 95.44% specificity. These findings suggest that the proposed algorithm effectively addresses class imbalance in medical image datasets, offering a robust solution for brain tumor classification. The particle rider mutual information-based classifier shows promise for enhancing diagnostic accuracy in clinical settings, demonstrating the efficacy of hybridized bio-inspired algorithms in managing imbalanced datasets.

This is an open access article under the [CC BY-SA](https://creativecommons.org/licenses/by-sa/4.0/) license.



Corresponding Author:

Rahul Ramesh Chakre
School of Computational Sciences, Faculty of Science and Technology, JSPM University Pune
Pune, Maharashtra, India
Email: rahulrchakre@gmail.com

1. INTRODUCTION

Due to the use of various imaging modalities in the medical field, the amount of medical image datasets is increasing rapidly [1]. Medical image analysis aids in diagnosing various illnesses. Due to its size, structure, and shape, multidimensional medical image analysis becomes a crucial task. The most common reason for cancer-related mortality is a brain tumor. Early diagnosis of this condition greatly increases the likelihood that the patient will receive a successful course of therapy and lowers the risk of life. Artificial intelligence and various optimization techniques are used to extract useful knowledge from the large medical image dataset in a way that medical practitioners will get help to diagnose the patients [2], [3]. The typical classification techniques presuppose that the dataset of medical images contains samples with a fair

distribution. The term “imbalanced dataset” refers to situations in which the distribution is not fair. This type of dataset will cause biased learning, which results in an ineffective model [4], [5]. The imbalanced dataset is nothing more than an uneven distribution of samples across classes [6]. In this, there are more samples of one class than another. In the end, the class with the most samples will be the major class, and the class with the fewest samples will be the secondary class. In many real-world applications, including detecting fraud, brain tumors, intrusion detection systems, and entity resolution, the imbalanced distribution problem is present [7], [8]. Effective feature extraction, feature selection, and feature classification approaches are required for computer-aided diagnosis employing multidimensional images.

Due to the low number of important data instances, imbalanced data distribution problems arise when the majority class segment has a higher proportion than the minority class segment [9]. Numerous real-world applications, such as text classification, defect detection, fraud detection, oil spill detection in satellite pictures, toxicology, cultural modeling, and medical diagnostics, are plagued by the imbalanced data set problem [10]. The following factors contribute to the current classification algorithms' inadequate performance on imbalanced data sets: i) They are accuracy-driven, i.e., they strive to reduce the overall error, of which the minority class makes up a very small portion; ii) They make the supposition that the data is distributed equally across all classes; and iii) They likewise presume that errors originating from various categories have the same cost [11]. Both at the data and algorithmic levels, a variety of approaches to the imbalance dataset problem have already been put forth. These approaches include a variety of re-sampling techniques at the data level, including random oversampling with replacement, random under-sampling, directed oversampling, directed under-sampling, oversampling with informed generation of new samples, and combinations of the techniques. When working with decision trees, modifying the probability estimate at the tree leaf, adjusting the decision threshold, and recognition-based rather than discrimination-based learning are some algorithmic strategies that address the class imbalance [12]. Most classifiers, including decision trees and neural networks, perform well when the dataset's response variable distribution is balanced but it suffers from the problem of imbalance [13]. Input data sampling is regarded as a popular method of correcting data imbalance. It modifies the structure of the real data set to change its balancing ratio to the desired level by using both under-sampling and oversampling [14].

As mentioned in the introduction, unequal distribution of samples causes biased learning and directly affects the worthiness of the model. However, we could conclude that training on the imbalanced dataset has a significantly weak impact on the performance, so it is necessary to investigate new techniques for verifying the performance on the imbalanced dataset. Most of the techniques are analyzed using the balanced dataset i.e. more or less equal distribution of classes. So, an efficient performance on an imbalanced magnetic resonance image dataset is a very challenging task. Analysis of multivariate medical imaging is an important task, as was said in the introduction. Brain tumors cause most cancer-related fatalities. The likelihood that a patient would receive an effective therapy is significantly increased by early diagnosis of certain disorders. The proposed solution is “hybridization of particle rider mutual information and dendritic cell squirrel search algorithm with artificial immune classifier (AIC) for brain tumor classification for imbalanced magnetic resonance image dataset”.

The goal of this research is to analyze particle rider mutual information (PRMI) and dendritic cell squirrel search algorithm (DCA-SSA) with an AIC [15] for brain tumor classification on an imbalanced magnetic resonance image dataset. Region of interest and Gaussian filters are used to eliminate noise and artifacts from the image. To acquire segments, sparse fuzzy C-means clustering (Sparse FCM) [16] has also been utilized. Each segment's statistical and texture data are combined to form a feature vector. The PRMI [17], which was created by fusing the particle swarm optimization (PSO) [18], rider optimization algorithm (ROA) [19], and mutual information (MI), is utilized for feature selection. AIC induces the chosen features to identify the tumorous regions [20]. The artificial immune classifier is trained using the DCA-SSA method [21], which combines the squirrel search technique (SSA) [22] and the dendritic cell algorithm (DCA) [23]. The recommended DCA-SSA method is used to improve the artificial immune classifier parameters [24].

2. METHOD

As shown in Figure 1, this paper offers performance analysis for the brain tumor classification method named dendritic cell-squirrel search algorithm-based classifier on imbalanced medical image dataset. An experimental result shows that the proposed algorithm gives promising results on the imbalanced medical image dataset. Here, the preprocessing of the input MR image is carried out with the help of the region of interest and Gaussian filter. The preprocessed image is given towards the sparse fuzzy C-means for the segmentation task. Statistical features and local derivative patterns (LDP) are extracted from the segmented image. Following that, the feature selection process is accomplished by combining three algorithms: mutual information, rider optimization technique, and PSO. The integration of the squirrel search algorithm with dendritic cell algorithm completes the classification.

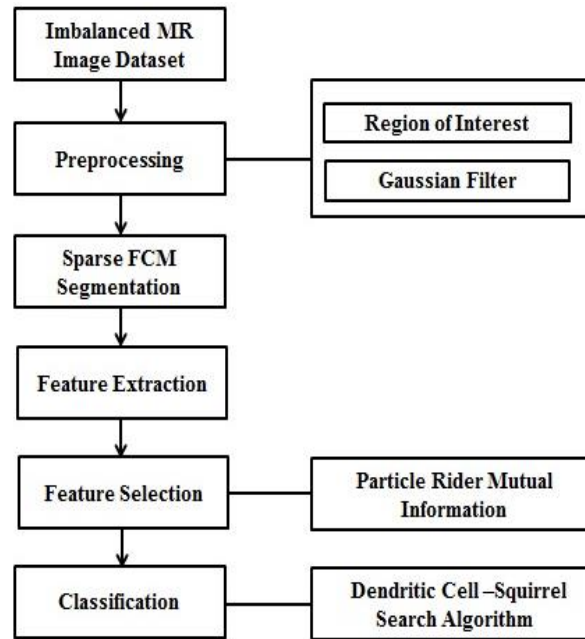


Figure 1. Block diagram of hybrid classification method

2.1. Input brain MR image

Suppose the imbalanced dataset M with the total number of k samples. The expression for the dataset with the quantity of images is shown (1).

$$M = \{m_1, m_2, \dots, m_i, \dots, m_k\} \quad (1)$$

Here, m_i states the i^{th} MR image in the dataset and the total number of samples in the dataset is represented as m_k .

2.2. Pre-processing of MR image

The removal of undesirable distortions from the image during pre-processing, which is a crucial step in classifying brain tumors, is performed using the region of interest and Gaussian filter.

a. Region of interest

By considering successive masking, the region of interest is frequently determined from the values of pixel intensities. The determination of continuous pixels having a value of 1 and excluding the value of 0 is a vital step in the region of interest extraction process. The values of the region of interest intensity are commonly referred to as density slices.

b. Gaussian filter

The Gaussian filter is frequently used to remove noise and it can provide a smooth transition. The Gaussian two-dimensional distribution is as (2).

$$G(x, y) = \frac{1}{\sqrt{2\pi\sigma^2}} e^{-\frac{x^2+y^2}{2\sigma^2}} \quad (2)$$

Here, σ states the standard deviation while x and y characterize the dimension of the kernel. The pre-processed output acquired after filtering the image is identified as Q_i .

2.3. Segmentation of preprocessed image

The pre-processed output Q_i is given input to the segmentation process, which is performed using sparse fuzzy C-means clustering, and it is developed by the modification of typical fuzzy C-means clustering. Utilizing sparse fuzzy C-means clustering offers high dimensional data clustering, which is the main benefit. The following actions are taken when using sparse fuzzy C-means clustering:

- a. Initialization: Initially, the feature weights are stimulated and are represented as $\omega = \omega_1^r = \omega_2^r = \dots = \omega_b^a = \frac{1}{\sqrt{b}}$. The features attained from pixel position are assumed as $b = 2$.

b. Updation of partition matrix: At first, the attribute weights ω and cluster center K when $\varepsilon(\mathfrak{N})$ is minimized,

$$C_{lm} = \begin{cases} \frac{1}{N_m}; & \text{if } P_{lm} = 0 \text{ and } N_t = \text{card}\{1: P_{lm} = 0\} \\ 0; & \text{if } P_{lm} \neq 0 \text{ but } P_{lg} = 0 \text{ for some } g, g \neq m \\ \frac{1}{\sum_{g=1}^e \left(\frac{P_{lm}}{P_{gm}}\right)^{\left(\frac{1}{\alpha-1}\right)}}; & \text{otherwise} \end{cases} \quad (3)$$

c. Update cluster center K : Let us assume that ω and η be fixed and $\varepsilon(K)$ is minimized if

$$B_{kt} = \begin{cases} 0; & \text{if } \omega_t = 0 \\ \frac{\sum_{i=1}^g C_{lm}^{\alpha} \cdot F_{lt}}{\sum_{l=1}^g C_{lm}^{\alpha}}; & \text{if } \omega_t \neq 0 \end{cases} \quad (4)$$

Here, the weight component is represented as t and k .

d. Evaluate the class: The class value is evaluated with constant clusters $Seg_i = \{Seg_1, Seg_3, \dots, Seg_{ii}, \dots, Seg_n\}$ and membership B .

e. Terminate: The steps are continued until it reaches the satisfied criterion. The outcome of sparse fuzzy C-means clustering depicted the segments received from the pre-processed image and it is shown (5).

$$Seg_i = \{Seg_1, Seg_3, \dots, Seg_{ii}, \dots, Seg_n\} \quad (5)$$

2.4. Feature extraction

To refine the relevant features for subsequent processing, feature extraction is a crucial step. Here, statistical features mean (f_1), variance (f_2), standard deviation (f_3), kurtosis (f_4), skewness (f_5), and energy (f_6) successfully extracted along with this texture feature LDP (f_7) is also extracted. Formation of feature vector.

$$F = \{f_1, f_2, f_3, f_4, f_5, f_6, f_7\} \quad (6)$$

2.5. Feature selection

The feature vector specified in (6) is subjected to the feature selection stage. Here, PRMI is used to select the most relevant feature. This algorithm is developed by the combination of PSO, ROA, and mutual information. The steps for the feature selection are as follows:

a. Initialization: Initialization is carried out by four groups of riders, scattered over a dimensional space, and shown as (7).

$$s = \{S_1, S_2, \dots, S_m, \dots, S_n\} \quad (7)$$

Here, S_n indicates the total number of solutions and S_m represents m^{th} solution.

b. Establish the fitness function

The recently developed objective function primarily relies on MI [16], which calculates the relationship between characteristics and class labels. The notion of "mutual information" is provided by $P(X, Y)$. The description of MI between two features and class label X and Y whose joint distribution is described by $P(X, Y)$ is expressed as (8).

$$R(X; Y) = \sum_{x \in X} \sum_{y \in Y} P(x, y) \log \frac{P(x, y)}{P(x) \cdot P(y)} \quad (8)$$

where, $P(X)$ and $P(Y)$ indicate marginal distributions of X and Y generated by the marginalization process. Here, the X indicates the features and Y represent the class labels.

c. Evaluation of weights

According to the ROA, the attacker's location is updated to choose the best course of action. By assuming the actions of each rider, as defined below, the rider upgrades its location. The position of the follower's improvement depends on the leading rider's ability to reach the goal and is as (9).

$$S_{t+1}^{follow}(z, p) = S^Y(Y, P) + [Cos(L_{y,p}^w * S^Z(Y, P) * D_z^w)] \quad (9)$$

where, Φ is coordinate selector, S^Y denote the position of the leading rider, Y specifies the index of the leading rider, $L_{p,w}^w$ indicates the steering angle of z^{th} rider in w^{th} coordinate, and D_z^w is the distance.

The updated position of the over taker is used in the update process for maximizing the success rate by determining the position of the over taker and is given by (10).

$$S_{w+1}^o(z, p) = S_w(z, p) + [\delta_w^*(p) * S^Z(Y, \Phi)] \quad (10)$$

where, $\delta_w^*(z)$ represent the direction indicator.

The bypass riders follow a common path without tracking the leading rider. In this context, the update rule of the bypass riders is exhibited in which the standard bypass rider is given as (11).

$$S_{w+1}(z, n) = \beta [S_w(\mu, n) \times \Delta(n) + S_w(\eta, n) * [1 - \Delta(n)]] \quad (11)$$

The proposed PRMI's final upgrade equation is as (12).

$$S_{w+1}(z, n) = \frac{(S_w(z, n)(K_1 H_1 + K_2 H_2 - 1) - J F_w(z, n) - K_1 H_1 E_w(z, n))(1 + \cos(L_{z, n}^w)) + D_z^w K_2 H_2}{K_2 H_2 - 1 - \cos(L_{z, n}^w)} \quad (12)$$

- d. Terminate: The stages are repeated until the best solution is discovered.

2.6. Brain tumor classification using artificial immune classifier-dendritic squirrel search algorithm

This section explains the classification of brain tumors, which is done using an AIC and dendritic squirrel search algorithm to fine-tune the classifier's weights. When dendritic cell algorithm and squirrel search algorithm are combined, the result is the produced dendritic-SSA. The result of this classification process is referred to as. The main idea behind this AIC is that it considers the immune system's background network when teaching the ideas of artificial intelligence system (AIS), which is defined as a machine learning mechanism. The main advantage of AIC is that no additional support is needed for parameter optimization. However, the main problem with conventional AICs is antibody population production. The steps are as follows,

- a. Initialization: The activation of weights and their associated parameters is the first stage.

$$X = \{X_1, X_2, \dots, X_z, \dots, X_y\} \quad (13)$$

Here, X_x is the location of z^{th} solution and y shows the overall solutions.

- b. Error determination: The mean squared error (MSE), displayed below, is the best solution discovered based on the fitness measure.

$$MSE = \frac{1}{i} \sum_{j=1}^i [X_j - O_j]^2 \quad (14)$$

Here, the expected result and the outcome achieved employing AIC is signified as X_j and O_j , respectively.

- c. Estimation of the modified equation: Utilizing created dendritic-SSA, the parameters of AIC are properly set to identify the tumorous region of the brain. Each antigen is appropriately detected in this algorithm by an antibody, and each connection of antibody-using agents is updated as (15).

$$X_{z,y}(S+1) = \frac{1 - P_t Q_w}{\gamma - P_t Q_w} \left[\gamma X_{z,y}(S+1) - \frac{P_t Q_w X_{zy}(S)(1-\gamma)}{1 - P_t Q_w} \right] \quad (15)$$

- d. Re-evaluating the solution given the error: The error is calculated using (15) and the algorithm generates less error and is utilized for training AIC.
- e. End: Once the optimal biases have been found, the process is repeated until the required number of iterations has been reached.

3. RESULTS AND DISCUSSION

This section elaborates on the performance analysis of existing the PSO+NSA, PSO+CSA, ACO+NSA, ACO+CSA, ABC+NSA, ABC+CSA techniques along with proposed ROA+dendritic-SSA AIC [9] and particle rider MI+dendritic cell-SSA-based AIC techniques utilizing an imbalanced dataset for learning and classification of brain tumors using accuracy, sensitivity, and specificity as performance measures along with time complexity analysis.

The study is carried out using increasing sample size training data. Input data sampling is the common solution for the imbalanced image dataset, it adjusts the structure of the real data set to change its balance ratio to the desired level by both under and over-sampling [10]. Additionally, the efficiency of particle rider MI+dendritic cell-SSA-based AIC for imbalanced BRATS and SimBRATS datasets is also examined. As mentioned earlier, in the preliminary investigation, we have applied data sampling on implicitly generated imbalanced BRATS and SimBRATS MRI dataset. Sampling has been done in percentages from 40% to 90% while increasing the sample size by 10%. The imbalanced dataset generated is used for experimentation with sampling and without sampling. The detailed dataset description is given in the next section.

3.1. Dataset description

Using imbalanced BRATS and simulated BRATS datasets, the particle rider MI+dendritic cell-SSA-based AIC is tested in terms of accuracy, sensitivity, and specificity. The datasets for BRATS and simulated BRATS were taken from BRATS 2015 [25], which presents images with varied degrees of severity. 30 patients' brain MRIs are taken into consideration from the BRATS database. Each patient's image is gathered here using four different modalities, including T1, T1C, T2, and FLAIR. For the study, 130–176 brain slices are produced by each modality. This dataset of MR images has been purposely imbalanced. A total of 1,728 brain MR images with various degrees of brain tumor severity were taken from the BRATS dataset for 30 patients, of which 1,256 were tumorous and 472 were not. Like this, the SimBRATS dataset contains information on 50 patients, including 124 MR images with varied degrees of brain tumor severity, of which 96 are tumorous and 28 are non-tumorous.

3.2. Evaluation metrics

The performance of both existing and proposed techniques is thoroughly explored by utilizing accuracy, sensitivity, and specificity as significant performance measures. This evaluation is supervised explicitly on the imbalanced BRATS and SimBRATS datasets, which are confronting due to their fundamental class imbalances. By concentrating on these metrics, the evaluation specifies an inclusive identification of how effectively each method performs in handling the complexities of these datasets.

3.3. Comparative analysis

3.3.1. Experimentations using sampled data

The comparative analysis of existing techniques namely PSO+NSA, PSO+CSA, ACO+NSA, ACO+CSA, ABC+NSA, ABC+CSA along with proposed ROA+dendritic SSA AIC and particle rider MI+dendritic cell-SSA-based AIC with accuracy, sensitivity, and specificity parameters is evaluated for the sampled imbalanced dataset which is mentioned earlier in the experimental results and discussion section. As shown in Table 1, proposed approaches, including PSO+DCA, ROA+dendritic-SSA based AIC, and PRMI+dendritic-SSA based AIC, get excellent accuracy scores (91.79% to 96.25%) towards the higher end of the training data percentages (70% to 90%), demonstrating their usefulness. The accuracy ratings of the four approaches, PSO+CSA and ACO+CSA, vary significantly when compared to various training data percentages. This shows that the amount of training data may have a greater impact on how well these strategies perform.

As shown in Table 2, proposed approaches, notably PSO+DCA, ROA+dendritic-SSA based AIC, and PRMI+dendritic-SSA based AIC, produce high sensitivity values (89.95% to 94.33%) at the higher end of the training data percentages (70% to 90%). This suggests that these techniques are particularly effective for detecting positive cases in the BRATS dataset. PRMI and PSO with DCA and dendritic-SSA based on AIC, these two techniques consistently exhibit exceptional sensitivity over all training data proportions, making them contenders for more exploration or application in circumstances where sensitivity is crucial.

Table 1. Accuracy analysis for brain tumor classification on the BRATS dataset using existing and proposed techniques with varying training data

| Imbalanced BRATS dataset training data in % | 40% | 50% | 60% | 70% | 80% | 90% |
|---|------------------|------------------|------------------|------------------|------------------|------------------|
| Methods | Accuracy for 40% | Accuracy for 50% | Accuracy for 60% | Accuracy for 70% | Accuracy for 80% | Accuracy for 90% |
| PSO+NSA | 73.31 | 74.45 | 75.21 | 76.43 | 79.92 | 81.32 |
| PSO+CSA | 72.86 | 73.16 | 74.47 | 77.07 | 79.76 | 86.5 |
| ACO+NSA | 73.38 | 78.5 | 80.42 | 82.12 | 85.46 | 88.99 |
| ACO+CSA | 75.68 | 80.57 | 80.72 | 81.79 | 86.71 | 89.03 |
| ABC+NSA | 77.62 | 81.75 | 84.52 | 85.45 | 88.09 | 91.35 |
| ABC+CSA | 79.2 | 83.64 | 86.45 | 88.28 | 89.02 | 92.55 |
| PSO+DCA | 82.41 | 84.53 | 90.66 | 91.79 | 92.92 | 94.06 |
| ROA+dendritic-SSA-based AIC | 85.5 | 87.63 | 90.75 | 91.88 | 93.02 | 94.85 |
| PRMI+dendritic-SSA-based AIC | 88.6 | 89.72 | 90.85 | 91.98 | 93.11 | 96.25 |

Table 2. Sensitivity analysis for brain tumor classification on the BRATS dataset using existing and proposed techniques with varying training data

| Imbalanced BRATS dataset training data in % | 40% | 50% | 60% | 70% | 80% | 90% |
|---|---------------------|---------------------|---------------------|---------------------|---------------------|---------------------|
| Methods | Sensitivity for 40% | Sensitivity for 50% | Sensitivity for 60% | Sensitivity for 70% | Sensitivity for 80% | Sensitivity for 90% |
| PSO+NSA | 71.84 | 72.96 | 73.71 | 74.9 | 78.32 | 79.69 |
| PSO+CSA | 71.41 | 71.7 | 72.98 | 75.53 | 78.17 | 84.77 |
| ACO+NSA | 71.91 | 76.93 | 78.81 | 80.48 | 83.75 | 87.21 |
| ACO+CSA | 74.17 | 78.96 | 79.1 | 80.15 | 84.97 | 87.25 |
| ABC+NSA | 76.07 | 80.11 | 82.83 | 83.74 | 86.33 | 89.53 |
| ABC+CSA | 77.62 | 81.96 | 84.72 | 86.52 | 87.24 | 90.7 |
| PSO+DCA | 80.76 | 82.84 | 88.85 | 89.95 | 91.06 | 92.17 |
| ROA+dendritic-SSA-based AIC | 83.79 | 85.87 | 88.94 | 90.05 | 91.16 | 92.96 |
| PRMI+dendritic-SSA-based AIC | 86.82 | 87.93 | 89.03 | 90.14 | 91.25 | 94.33 |

As shown in Table 3, proposed approaches, notably PSO+DCA, ROA+dendritic-SSA based AIC, and PRMI+dendritic-SSA based AIC produce elevated specificity values (91.88% to 94.85%) at the higher end of the training data percentages (70% to 90%). These techniques are consistent for detecting true negative cases. PRMI and ROA and dendritic-SSA based AIC. These approaches consistently exhibit exceptional specificity in all training data proportions, according to AIC, making them suitable options for applications where specificity is important.

Table 3. Specificity analysis for brain tumor classification on the BRATS dataset using existing and proposed techniques with varying training data

| Imbalanced BRATS dataset training data in % | 40% | 50% | 60% | 70% | 80% | 90% |
|---|---------------------|---------------------|---------------------|---------------------|---------------------|---------------------|
| Methods | Specificity for 40% | Specificity for 50% | Specificity for 60% | Specificity for 70% | Specificity for 80% | Specificity for 90% |
| PSO+NSA | 73.38 | 74.53 | 75.29 | 76.51 | 79.99 | 81.4 |
| PSO+CSA | 72.94 | 73.24 | 74.54 | 77.15 | 79.84 | 86.58 |
| ACO+NSA | 73.45 | 78.58 | 80.5 | 82.2 | 85.55 | 89.08 |
| ACO+CSA | 75.76 | 80.65 | 80.8 | 81.87 | 86.79 | 89.12 |
| ABC+NSA | 77.7 | 81.83 | 84.6 | 85.54 | 88.18 | 91.44 |
| ABC+CSA | 79.28 | 83.72 | 86.53 | 88.37 | 89.11 | 92.64 |
| PSO+DCA | 82.49 | 84.62 | 90.75 | 91.88 | 93.01 | 94.15 |
| ROA+dendritic-SSA-based AIC | 85.59 | 87.71 | 90.84 | 91.98 | 93.11 | 94.95 |
| PRMI+dendritic-SSA-based AIC | 88.68 | 89.81 | 90.94 | 92.37 | 93.13 | 94.85 |

As shown in Table 4, the accuracy percentage for different methods applied to the imbalanced SimBRATS dataset with training data ranging from 40% to 90%. "PRMI+dendritic-SSA-based AIC" attains superior accuracy, attainment from 96.35% at 90% training data. "PSO+NSA" steadily has the lowermost accuracy, refining from 70.38% to 78.4% as training data increases.

As shown in Table 5, the sensitivity percentage for methods on the imbalanced SimBRATS dataset with training data is from 40% to 90%. "PRMI+dendritic-SSA-based AIC" attains superior sensitivity, reaching 94.42% with 90% training data. "ROA+dendritic-SSA-based AIC" also performs highly, with sensitivity rising from 82.88% to 92.05%. "ABC+CSA" and "ABC+NSA" exhibit robust sensitivity advances, reaching up to 90.79% and 88.62%, correspondingly, at 90% training data. "PSO+DCA" and "ACO+CSA" also exhibit prominent sensitivity gains, realizing 92.27% and 87.34% at 90% training data. "PSO+NSA" continues as the least sensitive method, progressing from 69.97% to 79.83% with more training data.

As shown in Table 6, the specificity percentage for different methods on the imbalanced SimBRATS dataset, with training data ranging from 40% to 90%. "PRMI+dendritic-SSA-based AIC" steadily attains superior specificity, reaching 95.44% at 90% training data. "ROA+dendritic-SSA-based AIC" comprehends intently, with specificity increasing from 85.67% to 94.04% as training data expands. "ABC+CSA" and "ABC+NSA" also show considerably strong performance, with specificity going up to 91.73% and 90.54%, correspondingly, at 90% training data. "PSO+DCA" exhibits substantial advancement, accomplishing 92.24% specificity at 90% training data. "ACO+CSA" and "ACO+NSA" reach up to 90.47% and 89.16% specificity, correspondingly. "PSO+NSA" has minimal specificity but still adjusts from 70.45% to 78.48% as training data increases. The results show a typical inclination of increasing specificity as the percentage of training data increases for all methods. This implies that each method is more precise in appropriately identifying negative instances with more training data. Methods especially integrating dendritic-SSA-based AIC, such as "PRMI+dendritic-SSA-based AIC" and "ROA+dendritic-SSA-based AIC," steadily outperform others, emphasizing their robustness in handling the imbalanced SimBRATS dataset.

Table 4. Accuracy analysis for brain tumor classification on the SimBRATS dataset using existing and proposed techniques with varying training data

| Imbalanced SimBRATS dataset training data in % | 40% | 50% | 60% | 70% | 80% | 90% |
|--|------------------|------------------|------------------|------------------|------------------|------------------|
| Methods | Accuracy for 40% | Accuracy for 50% | Accuracy for 60% | Accuracy for 70% | Accuracy for 80% | Accuracy for 90% |
| PSO+NSA | 70.38 | 71.53 | 72.29 | 73.5 | 76.99 | 78.4 |
| PSO+CSA | 72.94 | 73.24 | 74.54 | 77.15 | 79.84 | 84.58 |
| ACO+NSA | 73.45 | 78.58 | 80.5 | 82.2 | 85.55 | 89.08 |
| ACO+CSA | 75.76 | 80.65 | 80.8 | 81.87 | 86.79 | 89.12 |
| ABC+NSA | 77.7 | 81.83 | 84.6 | 85.54 | 88.18 | 91.45 |
| ABC+CSA | 79.28 | 83.72 | 86.53 | 88.37 | 89.11 | 92.64 |
| PSO+DCA | 82.49 | 84.62 | 90.75 | 91.88 | 93.01 | 94.15 |
| ROA+dendritic-SSA-based AIC | 85.59 | 87.72 | 90.85 | 91.98 | 93.11 | 94.95 |
| PRMI+dendritic-SSA-based AIC | 88.68 | 89.81 | 90.94 | 92.07 | 93.21 | 96.35 |

Table 5. Sensitivity analysis for brain tumor classification on the SimBRATS dataset using existing and proposed techniques with varying training data

| Imbalanced SimBRATS dataset training data in % | 40% | 50% | 60% | 70% | 80% | 90% |
|--|---------------------|---------------------|---------------------|---------------------|---------------------|---------------------|
| Methods | Sensitivity for 40% | Sensitivity for 50% | Sensitivity for 60% | Sensitivity for 70% | Sensitivity for 80% | Sensitivity for 90% |
| PSO+NSA | 69.97 | 70.6 | 71.84 | 72.03 | 74.45 | 79.83 |
| PSO+CSA | 70.48 | 71.77 | 72.05 | 74.61 | 77.25 | 83.89 |
| ACO+NSA | 74.98 | 76.01 | 78.39 | 79.56 | 81.84 | 86.29 |
| ACO+CSA | 74.24 | 79.04 | 79.18 | 80.23 | 85.06 | 87.34 |
| ABC+NSA | 78.15 | 79.19 | 82.51 | 83.83 | 86.42 | 88.62 |
| ABC+CSA | 77.69 | 82.05 | 84.8 | 86.6 | 87.33 | 90.79 |
| PSO+DCA | 79.84 | 81.93 | 86.94 | 88.04 | 90.15 | 92.27 |
| ROA+dendritic-SSA-based AIC | 82.88 | 84.96 | 88.03 | 89.14 | 90.25 | 92.05 |
| PRMI+dendritic-SSA-based AIC | 86.91 | 87.01 | 88.12 | 90.23 | 91.34 | 94.42 |

Table 6. Specificity analysis for brain tumor classification on the SimBRATS dataset using existing and proposed techniques with varying training data

| Imbalanced SimBRATS dataset training data in % | 40% | 50% | 60% | 70% | 80% | 90% |
|--|---------------------|---------------------|---------------------|---------------------|---------------------|---------------------|
| Methods | Specificity for 40% | Specificity for 50% | Specificity for 60% | Specificity for 70% | Specificity for 80% | Specificity for 90% |
| PSO+NSA | 70.45 | 71.6 | 72.36 | 73.58 | 77.07 | 78.48 |
| PSO+CSA | 73.01 | 73.31 | 74.62 | 77.23 | 79.92 | 84.66 |
| ACO+NSA | 73.53 | 78.66 | 80.58 | 82.28 | 85.63 | 89.16 |
| ACO+CSA | 75.84 | 80.73 | 80.88 | 81.95 | 86.88 | 90.47 |
| ABC+NSA | 77.78 | 81.91 | 84.69 | 85.62 | 88.27 | 90.54 |
| ABC+CSA | 79.36 | 83.8 | 86.62 | 88.46 | 89.2 | 91.73 |
| PSO+DCA | 82.58 | 84.7 | 90.84 | 91.97 | 93.11 | 92.24 |
| ROA+dendritic-SSA-based AIC | 85.67 | 87.8 | 90.94 | 92.07 | 93.2 | 94.04 |
| PRMI+dendritic-SSA-based AIC | 88.77 | 89.9 | 91.03 | 92.16 | 93.3 | 95.44 |

3.3.2. Experimentations using K-fold cross validation on imbalanced dataset

Table 7 shows the outcomes of 10-fold analyses for different techniques on the BRATS and SimBRATS datasets. For each approach on both datasets, the accuracy (ACC), sensitivity (SEN), and specificity (SPE) percent are included in this analysis. The 10-fold analysis, outcomes reveal that the PRMI+dendritic-SSA-based AIC method reliably outperforms others on both the imbalanced BRATS and imbalanced SimBRATS datasets, attaining the maximum accuracy (96.25% and 96.35%, respectively) along with admirable sensitivity and specificity (around 94-95%). Other methods like PSO+DCA and ROA+dendritic-SSA-based AIC also demonstrate robust performance with accuracies over 94%, but they fall short compared to PRMI+dendritic-SSA. Methods such as ABC+CSA and ACO+CSA exhibit extensive enhancements over PSO+NSA and PSO+CSA, with accuracies varying from 89% to over 92%, indicating robust classification competencies. Overall, the PRMI+dendritic-SSA-based AIC method proves to be advanced, exhibiting superior classification accuracy and sensible sensitivity and specificity through both datasets.

Here is a summary of the findings: The approaches regularly perform well in terms of accuracy, sensitivity, and specificity for the BRATS dataset. With a 96.25% accuracy rate, PRMI+dendritic-SSA-based AIC has the best accuracy. The maximum sensitivity is PRMI+dendritic-SSA-based AIC, with values ranging from 79.69% to 94.33%. The range of specificity values is 81.4% to 94.85%, with the highest specificity being PRMI+dendritic-SSA-based AIC. The methods on the SimBRATS dataset perform well regarding accuracy, sensitivity, and specificity, just as the BRATS dataset. On this dataset as well, PRMI+dendritic-SSA-based

AIC obtains an excellent accuracy of 96.25%. The maximum sensitivity is PRMI+dendritic-SSA-based AIC, with values ranging from 79.69% to 94.33%. The range of specificity values is 81.4% to 94.85%, with the highest specificity being PRMI+dendritic-SSA-based AIC.

Table 7. K-fold analysis on imbalanced BRATS and SimBRATS dataset when K=10 for ACC (accuracy), SEN (sensitivity) and SPE (specificity) as performance measures

| 10-Fold analysis/methods K=10 | Imbalanced BRATS dataset | | | Imbalanced SimBRATS dataset | | |
|----------------------------------|--------------------------|---------|---------|-----------------------------|---------|---------|
| | ACC (%) | SEN (%) | SPE (%) | ACC (%) | SEN (%) | SPE (%) |
| PSO+NSA | 81.32 | 79.69 | 81.4 | 78.40 | 79.83 | 78.48 |
| PSO+CSA | 86.5 | 84.77 | 86.58 | 84.58 | 83.89 | 84.66 |
| ACO+NSA | 88.99 | 87.21 | 89.08 | 89.08 | 86.29 | 89.16 |
| ACO+CSA | 89.03 | 87.25 | 89.12 | 89.12 | 87.34 | 90.47 |
| ABC+NSA | 91.35 | 89.53 | 91.44 | 91.45 | 88.62 | 90.54 |
| ABC+CSA | 92.55 | 90.7 | 92.64 | 92.64 | 90.79 | 91.73 |
| PSO+DCA | 94.06 | 92.17 | 94.15 | 94.15 | 92.27 | 92.24 |
| ROA+dendritic-SSA-based AIC | 94.85 | 92.96 | 94.95 | 94.95 | 92.05 | 94.04 |
| PRMI+dendritic-SSA-based AIC | 96.25 | 94.33 | 94.85 | 96.35 | 94.42 | 95.44 |

3.3.3. Comparative discussion

For this experimentation, the imbalanced dataset is generated from BRATS and SimBRATS. The imbalanced dataset generated is used for experimentation with sampling and without sampling. As a primary investigation on an imbalanced image data set; to validate whether training data size affects the classification performance, we have randomly sampled the images from the dataset into 40% samples to 100% samples while increasing the sample size by 10% at each step. The results are presented in Tables 1 to 6 and graphically represented in Figures 2 and 3. It is found that as the size of the data sample is increased the classification performance also increases. So, it is concluded that we need to use all available samples in an imbalanced image data set for classification.

As a final investigation of our proposed method to handle an imbalanced image dataset, we have applied a completely imbalanced dataset (without sampling) to existing as well as proposed techniques. The results are shown in Table 7 with 10-fold cross-validation. Table 8 illustrates the results mainly using the proposed ROA+dendritic cell-SSA-based AIC and particle rider MI+dendritic cell-SSA-based AIC for imbalanced BRATS and SimBRATS dataset. The results using existing techniques namely PSO+NSA, PSO+CSA, ACO+NSA, ACO+ CSA, ABC+NSA, and ABC+CSA are also presented in Table 8. It is found that the performance of existing techniques namely PSO+NSA, PSO+CSA, ACO+NSA, ACO+ CSA, ABC+NSA, and ABC+CSA is lower on imbalanced dataset whereas the proposed methods ROA+dendritic SSA AIC [9] and particle rider MI+dendritic cell-SSA-based AIC the dendritic cell-SSA-AIC has the better performance in terms of accuracy, sensitivity, and specificity when used with MRI for brain tumor classification.

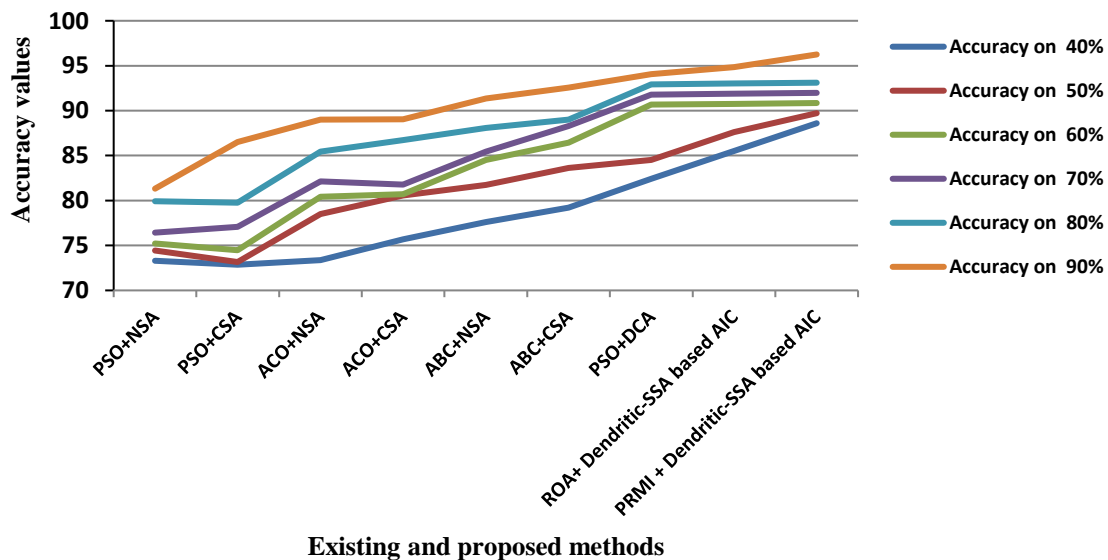
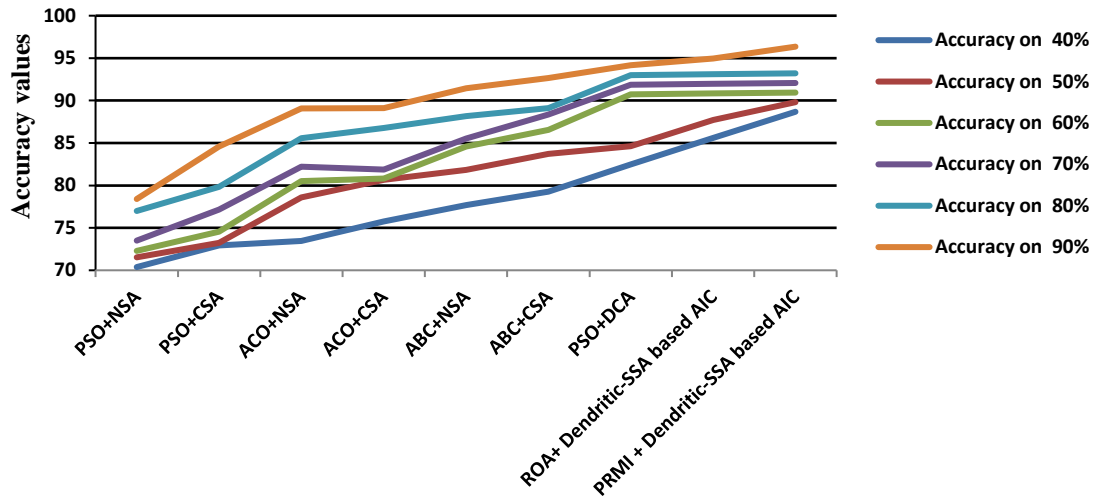


Figure 2. Analysis of existing and proposed methods using imbalanced BRATS dataset



Existing and proposed methods

Figure 3. Analysis of existing and proposed methods using imbalanced SimBRATS dataset

Table 8. Analysis of various performance measures using various methods for brain tumor image classification on imbalanced BRATS and SimBRATS datasets

| Methods | Imbalanced BRATS dataset | | | Imbalanced SimBRATS dataset | | |
|------------------------------|--------------------------|---------|---------|-----------------------------|---------|---------|
| | ACC (%) | SEN (%) | SPE (%) | ACC (%) | SEN (%) | SPE (%) |
| ROA+dendritic-SSA-based AIC | 94.85 | 92.96 | 94.95 | 94.95 | 92.05 | 94.04 |
| PRMI+dendritic-SSA-based AIC | 96.25 | 94.33 | 94.85 | 96.35 | 94.42 | 95.44 |

The most enhanced classification performance of around 96.25% accuracy is achieved due to training AIC classifiers with dendritic cell-SSA with particle rider MI, this method has a high convergence momentum and accuracy. Further, the computational complexity of segmentation based on sparse FCM is reduced. The particle rider MI's feature selection method selects the most informative features, resulting in the highest classification accuracy in almost all methods. Furthermore, the AIC classifier is self-organizing and necessitates good characteristics. As a result, the new strategy of taking the imbalanced dataset improves overall speed while reducing errors. Similarly, the second proposed method ROA+dendritic SSA AIC also gives similar results to particle rider MI+dendritic Cell-SSA with classification accuracy of around 94.85%. While the existing 7 methods provide a minimum of 81.32 to a maximum of 94.06 percent classification performance in terms of accuracy

As shown in Table 8, on both imbalanced datasets, both methods PRMI+dendritic-SSA based AIC and ROA+dendritic-SSA based AIC demonstrate strong performance. While both techniques maintain high levels of sensitivity, PRMI+dendritic-SSA-based AIC tends to have a minor advantage in terms of accuracy and specificity.

3.3.4. Analysis based on time

The methods on the unbalanced BRATS dataset have a wide range of execution times. Execution times for PSO+NSA, ABC+NSA, and ABC+CSA range from about 9.36 seconds to 10.64 seconds, which is comparatively long. Execution times for PSO+CSA, ACO+NSA, and ACO+CSA are reasonable, ranging from 5.64 to 6.50 seconds. The execution times of the algorithms PSO+DCA, ROA+dendritic-SSA based AIC, and PRMI+dendritic-SSA based AIC are all impressively fast—under 1 second. The algorithms' execution times on the imbalanced SimBRATS dataset vary as well. Execution times for PSO+NSA and ABC+NSA are relatively long, at about 8.21 and 7.19 seconds, respectively. The highest execution time of ABC+CSA is 7.84 seconds. ACO+NSA executes in a respectable 7.02 seconds. Execution timings for PSO+CSA, ACO+CSA, PSO+DCA, and ROA+dendritic-SSA-based AIC range from 2.88 seconds to 5.00 seconds. The fastest execution time for this dataset's PRMI+dendritic-SSA-based AIC is 0.88 seconds. Table 9 illustrates the analysis based on the required time for the execution while using the imbalanced dataset. It is observed that the two proposed methods ROA dendritic cell-SSA based AIC and particle rider MI+dendritic cell-SSA based AIC give better results in terms of lower execution time when compared with existing methods.

Table 9. Analysis based on time

| Methods/Dataset | Execution time in second | |
|--------------------------------|--------------------------|---------------------|
| | Imbalanced BRATS dataset | Imbalanced SimBRATS |
| PSO+NSA | 9.36 | 8.21 |
| PSO+CSA | 5.64 | 7.83 |
| ACO+NSA | 6.50 | 7.02 |
| ACO+CSA | 6.48 | 5.00 |
| ABC+NSA | 10.64 | 7.19 |
| ABC+CSA | 10.59 | 7.84 |
| PSO+DCA | 0.03 | 2.88 |
| ROA+ Dendritic-SSA-based AIC | 0.03 | 3.74 |
| PRMI + Dendritic-SSA-based AIC | 0.02 | 0.88 |

4. CONCLUSION

This study presents two proposed techniques for the classification of brain tumors on imbalanced datasets. The first one is ROA+dendritic cell-SSA based AIC and the second technique is particle rider MI+dendritic cell-SSA based AIC on an imbalanced MR imaging dataset. The experimental finding demonstrates that the strategies are effective in terms of performance metrics for classifying brain tumors. In both proposed methods, the process begins with noise and artifact removal from the input brain MR images by applying Gaussian filters and a region of interest. Subsequently, the segmentation process is applied using sparse fuzzy C-means clustering. After this step, the feature extraction is done to extract statistical characteristics and textural features. The preprocessing steps up to this step are common for both methods. As a next step, in the first proposed method ROA is used for feature selection. Whereas, in the next step, in the second proposed method the PRMI is used for feature selection. The PRMI is developed by combining the mutual information, ROA, and PSO. Finally, the AIC is applied for the classification of brain tumors for both proposed methods. The AIC is trained using the dendritic cell-SSA algorithm. The dendritic cell-SSA algorithm is a hybridization of the dendritic cell method and the squirrel search algorithm. The experimental results show that the proposed particle rider mutual information-based dendritic squirrel search algorithm-based AIC outperformed other models for the imbalanced BRATS MR image dataset and provided an accuracy of 96.25%, sensitivity of 94.33%, and specificity of 94.85%. Similarly, on the other hand, it also outperforms other models and provides an accuracy of 96.35%, sensitivity of 94.42%, and specificity of 95.44% for the imbalanced SimBRATS dataset.




REFERENCES

- [1] J. Li *et al.*, "Feature selection: A data perspective," *ACM Computing Surveys*, vol. 50, no. 6, pp. 1–45, Nov. 2018, doi: 10.1145/3136625.
- [2] R. Sharma and A. S. Bist, "Machine learning: A survey," *International Journal of Engineering Sciences and Research Technology*, vol. 4, no. 3, pp. 708–716, 2015.
- [3] A. Kilani, A. Ben Hamida, and H. Hamam, "Artificial intelligence review," in *Encyclopedia of Information Science and Technology, Fourth Edition*, IGI Global, 2018, pp. 106–119.
- [4] A. Fernández, S. del Río, N. V. Chawla, and F. Herrera, "An insight into imbalanced big data classification: Outcomes and challenges," *Complex & Intelligent Systems*, vol. 3, no. 2, pp. 105–120, Jun. 2017, doi: 10.1007/s40747-017-0037-9.
- [5] B. Krawczyk, "Learning from imbalanced data: Open challenges and future directions," *Progress in Artificial Intelligence*, vol. 5, no. 4, pp. 221–232, Nov. 2016, doi: 10.1007/s13748-016-0094-0.
- [6] G. Haixiang, L. Yijing, J. Shang, G. Mingyun, H. Yuanyue, and G. Bing, "Learning from class-imbalanced data: Review of methods and applications," *Expert Systems with Applications*, vol. 73, pp. 220–239, May 2017, doi: 10.1016/j.eswa.2016.12.035.
- [7] P. Branco, L. Torgo, and R. P. Ribeiro, "A survey of predictive modeling on imbalanced domains," *ACM Computing Surveys*, vol. 49, no. 2, pp. 1–50, Jun. 2017, doi: 10.1145/2907070.
- [8] L. Yi, D. Xing-chun, C. Jian-jun, Z. Xing, and S. Yu-ling, "A method for entity resolution in high dimensional data using ensemble classifiers," *Mathematical Problems in Engineering*, vol. 2017, no. 1, Jan. 2017, doi: 10.1155/2017/4953280.
- [9] A. Amin *et al.*, "Comparing oversampling techniques to handle the class imbalance problem: A customer churn prediction case study," *IEEE Access*, vol. 4, pp. 7940–7957, 2016, doi: 10.1109/ACCESS.2016.2619719.
- [10] S. Vajda and G. A. Fink, "Strategies for training robust neural network based digit recognizers on unbalanced data sets," in *2010 12th International Conference on Frontiers in Handwriting Recognition*, Nov. 2010, pp. 148–153, doi: 10.1109/ICFHR.2010.30.
- [11] C. V. K. Veni and T. S. Rani, "On the classification of imbalanced data sets," *International Journal of Computer Science and Technology*, vol. 2, no. 1, pp. 145–148, 2011.
- [12] N. V. Chawla, N. Japkowicz, and A. Kotcz, "Editorial: Special issue on learning from imbalanced data sets," *ACM SIGKDD Explorations Newsletter*, vol. 6, no. 1, pp. 1–6, Jun. 2004, doi: 10.1145/1007730.1007733.
- [13] J. Li, S. Fong, S. Mohammed, and J. Fiadh, "Improving the classification performance of biological imbalanced datasets by swarm optimization algorithms," *The Journal of Supercomputing*, vol. 72, no. 10, pp. 3708–3728, Oct. 2016, doi: 10.1007/s11227-015-1541-6.
- [14] T. M. Khoshgoftaar, A. Fazelpour, D. J. Dittman, and A. Napolitano, "Ensemble vs. Data sampling: Which option is best suited to improve classification performance of imbalanced bioinformatics data?," in *2015 IEEE 27th International Conference on Tools with Artificial Intelligence (ICTAI)*, Nov. 2015, pp. 705–712, doi: 10.1109/ICTAI.2015.106.
- [15] R. R. Chakre and D. V. Patil, "Particle rider mutual information and dendritic-squirrel search algorithm with artificial immune classifier for brain tumor classification," *The Computer Journal*, vol. 66, no. 3, pp. 743–762, Mar. 2023, doi: 10.1093/comjnl/bxab194.




- [16] X. Chang, Q. Wang, Y. Liu, and Y. Wang, "Sparse regularization in fuzzy C-means for high-dimensional data clustering," *IEEE Transactions on Cybernetics*, vol. 47, no. 9, pp. 2616–2627, Sep. 2017, doi: 10.1109/TCYB.2016.2627686.
- [17] E. G. Learned-Miller, "Entropy and mutual information," Department of Computer Science, University of Massachusetts, Amherst, MA, USA, 2013.
- [18] J. Wang, Y. Cao, B. Li, H. Kim, and S. Lee, "Particle swarm optimization based clustering algorithm with mobile sink for WSNs," *Future Generation Computer Systems*, vol. 76, pp. 452–457, Nov. 2017, doi: 10.1016/j.future.2016.08.004.
- [19] D. Binu and B. S. Kariyappa, "RideNN: A new rider optimization algorithm-based neural network for fault diagnosis in analog circuits," *IEEE Transactions on Instrumentation and Measurement*, vol. 68, no. 1, pp. 2–26, Jan. 2019, doi: 10.1109/TIM.2018.2836058.
- [20] M. Karakose, "Reinforcement learning based AIC," *The Scientific World Journal*, 2013.
- [21] J. Greensmith, U. Aickelin, and S. Cayzer, "Detecting danger: The dendritic cell algorithm," in *Robust Intelligent Systems*, London: Springer London, 2008, pp. 89–112.
- [22] M. Jain, V. Singh, and A. Rani, "A novel nature-inspired algorithm for optimization: Squirrel search algorithm," *Swarm and Evolutionary Computation*, vol. 44, pp. 148–175, Feb. 2019, doi: 10.1016/j.swevo.2018.02.013.
- [23] J. Greensmith, "The dendritic cell algorithm," Ph.D. dissertation, Intelligent Modeling and Analysis, School of Computer Science, University of Nottingham, UK, 2007.
- [24] M. Karakose, "Reinforcement learning based artificial immune classifier," *The Scientific World Journal*, vol. 2013, no. 1, Jan. 2013, doi: 10.1155/2013/581846.
- [25] "BraTS datasets taken," *smir.ch*, <https://www.smir.ch/BRaTS/Start2015> (accessed Feb. 01, 2019).

BIOGRAPHIES OF AUTHORS






Rahul Ramesh Chakre    received a Ph.D. degree in computer engineering from Savitribai Phule Pune University (SPPU), Pune, Maharashtra, India. He received a B.E. degree in information technology in 2011 from the Government College of Engineering Aurangabad, Maharashtra, India, and an M.E in computer science and engineering in 2014 from Dr. Babasaheb Ambedkar Marathwada University, Maharashtra, India. His areas of interest are swarm intelligence, immune computing algorithms, and machine learning. He can be contacted at email: rahulrchakre@gmail.com.



Archana S. Vaidya    received a Ph.D. degree in computer engineering from Savitribai Phule Pune University (SPPU), Pune, Maharashtra, India. She received her master's degree in computer engineering from V.J.T.I., Mumbai University (INDIA) in 2010 and bachelor's degree in computer engineering from Walchand College of Engineering Sangli Shivaji University (INDIA) in 2002. Her areas of interest are parallel computing and machine learning. She has teaching experience of 22 years. She is a life member of ISTE and IAENG. She has published 9 Scopus-indexed papers and 40+ journal papers. She can be contacted at archana.vaidya@ges-coengg.org.



Dipak V. Patil    received a B.E. degree in computer engineering in 1998 from the University of North Maharashtra India and an M.Tech. degree in computer engineering in 2004 from Dr. Babasaheb Ambedkar Technological University, Lonere, India. He has done a Ph.D. degree from S.R.T.M. University, Nanded. Currently, he is a professor and head of the Computer Engineering Department at GES R.H. Sapat College of Engineering, Management Studies and Research, Nashik, India which is affiliated with the Savitribai Phule Pune University, Pune, and Maharashtra, India 422002. He can be contacted at email: dipakvpatil17@gmail.com.